DUCTILE FRACTURE MECHANISMS OF STRUCTURAL STEELS

J. Lereim[1]

Ductile fracture mechanisms at initiation and subsequent stable crack growth are studied with particular reference to the behaviour of rolled structural steels where splitting is an important factor for the strain localization ahead of through thickness cracks. Damage models are established for the deformation behaviour prior to initiation of stable crack extension as well as for the actual propagation, when strain controlled conditions are present.

INTRODUCTION

In order to establish a physical understanding of the actual fracture toughness obtained, a detailed study is required of the local damage processes ahead of the crack tip. The present work concerns the ductile fracture mechanisms of rolled structural steels where the damage may be considered essentially as strain controlled for the initiation as well as the stable crack growth regime. The localized damage at initiation of crack extension is frequently described by some critical strain exceeded within some characteristic region a head of the crack tip, Smith and Knott (1). This region is described as the fracture process zone where the localized deformation is independent of the extent of the total plastic zone, but is a function of the straining path and volume fraction of second phase particles as well as the distance between inclusion bands in rolled plates, J. Lereim et al (2), Iricibar et al (3).

Therefore, the damage in the process zone prior to initiation of stable crack growth may be regarded as a characteristic of the material and proper models are required for further development. Similarly to the initiation problem, some kind of process zone is present ahead of the crack during stable crack growth. The latter may also be a characteristic of the material when assuming the local failure mechanism to be strain-controlled and the volume of the process zone is very small relative to the total plastic zone, E. Smith (4,5). Modelling of the local deformation in the advancing process zone should link the microstructural features with the observed behaviour.

1 Det norske Veritas, P.O. Box 300, N-1322 HØVIK, Oslo, NORWAY

MATERIALS AND EXPERIMENTAL PROCEDURE

The model materials used are the three ship hull steels of the grades NVA, NVD and NVE 36 according to the DnV Rules (6). Similar qualities are given in the Rules of Lloyds (7) and ABS (8), and the chemical composition is given in Table 1. The rolled plates to be tested were received from an ordinary steel supply store in order to examine randomly selected qualities of the various grades that are commenly used for ship structures.

The tensile properties were characterized in terms of uniaxial tensile testing and testing under plane strain conditions. The plane strain tensile speciméns were similar to those used by Clausing (9). The corresponding fracture toughness properties were obtained by using standard pure bend specimens of the preferred 2 x 1 type when referring to BS 5762: 1979 (10). The platethickness is 25 mm and full thickness specimens are sectioned in the LT and TL directions which are the important orientations when considering the risk of unstable fracture of through thickness cracks or defects.

The initiation toughness parameters in terms of $CTOD_i$ and J_{IC} were determined by the replication technique initially described by Robinson (11), and later applied by Fields and Miller (12) and used by Lereim and Embury (13) for single specimen $CTOD_i/J_{IC}$ testing.

TABLE 1 - Chemical composition of the steels examined

Quality \ weight %	C	Si	Mn	P	S	Ni	Cr	Al	N
NVA	0,12	0,16	0,48	0,017	0,021	<0,02	<0,02	<0,005	0,007
NVD	0,16	0,28	0,89	0,022	0,027	<0,02	<0,02	0,009	0,008
NVE 36	0,14	0,20	1,46	0,010	0,014	0,02	<0,02	0,044	0,007

RESULTS

Tensile properties.

Tensile properties of the steel are given in tables 2 and 3 for uniaxial and plane strain conditions respectively. Concerning the plane strain properties, testing was performed for the NVA grade steel only. The corresponding plane strain properties for the grades NVD and NVE 36 were derived from the uniaxial fracture strains and estimated ratios of the fracture strain under plane strain conditions and the corresponding uniaxial fracture strain. This ratio $\varepsilon_{fps}/\varepsilon_f$ was derived from the yield strength, using the mean line on fig 1, which includes the original data of Clausing (9) as well as data of Lereim and Embury (2) and Slatcher (14).

Fracture toughness

The ductile fracture resistance was for the present steels characterized by the toughness at initiation of stable crack growth, $CTOD_i$ and J_{IC}, and by the max load toughness $CTOD_u$. In general, the toughness properties in the LT-direction were better than in the TL-direction, particularly for the ultimate load toughness which may reflect a significicant difference in crack growth resistance prior to maximum load. The results are reported in table 4.

TABLE 2 - Uniaxial tensile test

Test temp.	Quality	Orien-tation	ε_f	ε_{UTS}	σ_y (N/mm^2)	σ_{UTS} (N/mm^2)	σ_f (N/mm^2)
23^{o}C	NVA	T	1.23	0.18	219.7	462.5	921.3
	NVA	L	1.23	0.19	207.6	449.8	913.0
	NVD	L	1.53		266.6		
	NVD	T	1.26		288.1		1050.6
	NVA	L	0.09	0.21	228.8	478.5	813.0

TABLE 3 - Plane strain tensile properties at room temperature

Quality	Orientation	Plane strain		"Uniaxail"
		ε_{UTSP}	ε_{fPS}	ε_f
NVA	Transverse, T through thickness	.16	.55	1.23
	Longitudinal, L through thickness	.19	.61	1.15
	Transverse, TP parallell plate	.19	.65	1.23
NVD	Transverse, T through thickness	.18	.82*	1.26
	Longitudinal, L Through thickness	.2	1.0*	1.53
NVE 36	Transvers, T through thickness	.18	.76*	1.26
	Longitudinal through thickness	.19	.66*	1.10

*Derived from ε_f when assuming $\varepsilon_{fPS}/\varepsilon_f \simeq .65$

TABLE 4 - Main Fracture Toughness test results

Tested at room temperature.

Grade	Specimen orientation	$CTOD_u$ (mm)	$CTOD_i$ (mm)	J_{ic} (Nmm/mm^2)
NVA	LT	2.2	.28	77
	LT	2.3	.30	80
	LT	2.1	.24	83
	TL	.6	.22	64
	TL	.86	.19	72
	TL	.79	.2	71
	TL	.81	.18	66
	TL	.63	.26	70
NVD	LT	1.68	.25	143
	LT	1.8	.37	130
	LT	1.72	.35	122
	TL	.46	.25	86
	TL	.51	.30	85
	TL	.51	.25	81
NVE 36	LT	1.18	.25	108
	TL	.22	.21	74
	TL	.16	.15	77
	TL	.31	.25	65
	TL	.17	.14	26

PROCESS ZONE DAMAGE MODEL

Initiation of stable crack growth.

The first model of the process zone in mild steel was introduced by Smith and Knott (1) where the initiation toughness $CTOD_i$ is related to the material parameters governed by the microstructure such as:

$$CTOD_i = \varepsilon_c \times l \qquad 1)$$

ε_c was assumed to be the true uniaxial tensile strain to failure and l to be the distance between sulphide inclusions.

A similar relation to equation 1) was later established by Lereim and Embury (2) for modelling the initiation toughness $CTOD_i$ in controlled rolled X-70 pipe line steels. However, in the latter approach, the size of the process zone described by l in Eqution 1) was rather the distance between bands of inclusions than the actual distance between the single sulphides. In addition, the critical fracture strain was found to be more of the type under plane strain conditions, ε_{fps}, which is in accordance with the actual stress and strain state ahead of the cracktip. When characterizing the fracture toughness of rolled steels, a high degree of anisotropy may be present and the fracture toughness in the ductile range may vary significantly depending on the orientation of the test specimens with respect to the rolling direction which is also the case for the present examined ship steels, Lereim et al (2) and Willoughby et al (15).

Therefore, the effect of orientation must be reflected in the model of the process zone if a unique physical interpretation is to be established for the damage prior to initiation of ductile tearing. An attempt to include the orientation effect in Equation 1) is done by Willoughby et al (15). Their conclusion is that the damage prior to ductile tearing is governed by a two dimensional process on planes normal to the crack front with no lateral blunting. However, for real rolled plates, the initial fatigue crack front may intersect inclusions. Consequently the deformation history prior to initiation is partly a 3 dimensional process, as blunting may occur along the crack front as well as between the inclusions where the final stage is a localized necking and shear fracture mechanism. This is particularly the case for the TL and LT orientations where the critical strain is initially reached in the plane normal to the crack plane and intersecting the crack plane at the tip of the blunt notch. The present situation is schematically shown in fig. 2.

The sketches in fig 2 simulate the delamination or tunnelling along inclusion bands which is occuring in TL and LT oriented specimens at a considerably smaller macroscopic deformation than the corresponding deformation, at initiation of stable crack growth. Prior to delamination, plane strain conditions are present ahead of the crack tip. When delamination or tunnelling occurs prior to initiation, the stress state changes locally to conditions closer to plane stress in between the splits. However, the corresponding local deformation between the splits at the crack tip is similar to the necking mechanism occuring in the plane strain tensile specimens. Plastic straining during necking is then occuring in the lateral direction, parallel to the crack front, and in the maximum stress direction normal to the crack plane only.

Initiation of stable crack growth is present when the local strain between the splits ahead of the crack tip exceeds the fracture strain under conditions close to plane strain deformation where the final separation happens by the some localized shear mechanism. This argument is supported by the work of Lereim and Saether (16) where the fracture appearance in the fracture toughness specimens and in the plane strain tensile specimens identical with respect to sheared coalesced voids and the angle of fracture planes relative to the maximum stress direction. A refined damage model is then established where the actual deformation history between splits at the crack tip is included. With reference to the plane strain tensile specimen, splitting and subsequent necking are introduced when the local strain in the maximum stress direction at the crack tip exceeds the ultimate tensile strain. Further straining in the neck occurs until the strain reaches the fracture strain at the tip of the blunt stretch zone, while the strain at the ends of the neck normal to the crack plane has achieved the ultimate tensile strain. Assuming the length of the neck or ligament ot be equal to the height of

splits, the strain distribution in the necked region at initiation of stable crack growth may be given as:

$$\varepsilon(x) = \varepsilon_{UTSP} + (\varepsilon_{fPS} - \varepsilon_{UTSP}) \frac{x^3}{(H/2)^3} \qquad 2)$$

ε_{fPS} : true fracture strain under plane strain conditions
ε_{UTSP} : true strain at ultimate strength in plane strain conditions
x : distance along height of split measured from top of splits. See fig. 3.
H : height of splits ≡ length of neck

The strain distribution following equation 2) is shown in fig. 3 toghether with actual measurements of the necked region of the splits, and equation 2) is a reasonable description of the variation in strain in the ligaments to the side of the crack plane. The corresponding cumlative displacement normal to the crack plane which is also equivalent to the crack tip opening desplacement, may then become as follows:

$$CTOD_i = 2 \int_0^{H/2} \varepsilon(x)\, dx \qquad 3)$$

Then the integrated CTOD is derived by introducing equation 2) into equation 3). This is in agreement with work by J.F. Knott (17), who argued that it should be integrated over a distance or volume considerably larger than associated with the size of voids around carbides. It gives:

$$CTOD_i = \frac{H}{4} (\varepsilon_{fPS} + 3\, \varepsilon_{UTSP}) \qquad 4)$$

Thus the fracture toughness at initiation of stable growth in terms of $CTOD_i$ is uniquely defined through Equation 4) where H is the height of the splits or necks normal to the crackplane which is a function of specimen orientation and distance between inclusion. H may be measured in optical micrographs of the plane normal to the crackplane and intersecting the crackplane at the blunt stretch zone. Further H may be related to the distance between the inclusion bands by, for example:

$$H = f \cdot l \qquad 5)$$

There f is a direction factor dependent on specimen orientation. Combination of 4) and 5) then gives:

$$CTOD_i = \frac{f \cdot l}{4} (\varepsilon_{fPS} + 3\, \varepsilon_{UTSP}) \qquad 6)$$

Again, the initiation toughness is simply related to the spacing between inclusion bands and the actual fracture strain of an unnotched tensile specimen.

The height of the splits were measured on planes from the TL- and LT-specimens of the three ship steels tested. The corresponding distance between inclusion bands which coincides with the width of the splits, were also determined, and the direction factor f was derived for the LT- and TL-directions respectively. The split heights and the corresponding widths vary significantly with a distribution density function close to a lognormal or weibull type, and the approximate mean values are given in table 5. Of particular note is that the direction factor f is almost identical for the three steels tested in the TL as well as in the LT directions. The direction factor for the TL-specimens was determined to be a value of roughly 3.8, while the

TABLE 5 - Splitting characteriztics of the steels studied.

Grade		Splitheight H (mm)*	Split width at crack front W (mm)	Inclusion band spacing 1 (mm)*	Orientation factor f = H/L
NVA	TL	.6	.15	.15	4
	LT	.8	.15	.15	5.3
NVD	TL	.6	.16	.16	3.75
	LT	.9	.16	.16	5.6
NVE 36	TL	.44	.12	.12	3.7
	LT	.56	.12	.12	4.7

* Approximate mean value

corresponding number for the LT-direction is around 5.2. Thus, the results may indicate that a constant relation exists between the splitheight ocurring and the corresponding spacing between inclusion bands. Furthermore, a derived $CTOD_i$ value is obtained through the application of Equation 6). The predicted variation in $CTOD_i$ for the steels tested is given in figs 4,5 and 6 when the measured variation in split height or distance between inclusion bands is included in equation 4) or 6).

The recorded values in initiation toughness are close to the mean values of the distributions presented in figs 4 - 6. Thus, the length parameter included in equation 4) or 6) should be given by it's mean value in order to relate the real ductile initiation toughness of rolled plates to one of the major microstructurally dependent parameters of the material. Further, the present damage model of ductile initiation may be applied to almost any kind of rolled steel plates, since the critical length parameter may even represent the distance between weak bands or planes in the microstructure which are not caused by sulphide inclusions. The latter is recently experienced in essentially sulphide free controlled rolled steel of grade X-65 where the similar initiation failure mechanism is present.

Stable crack growth

Ductile failure mechanisms include strain controlled damage ahead of a crack in stationary conditions as well as for a propagating crack. The stationary crack situation is present up to initiation of stable crack growth, as described in the previous section where initiation of stable crack extension occurs at a certain critical strain. For a strain controlled failure mechanism, further stable crack extension is obtained when the strain at the tip of the sharp advancing crack reaches the failure strain representing the local conditions ahead of the moving crack front.

Dealing with the damage processes in rolled plates where splitting appears, the mechanisms may be similar to the illustration given in fig 7. Initially, uniform plane strain deformation is present, as for any material containing a loaded crack until initiation of splitting. This is assumed to

happen when the local plastic strain at the crack tip exceeds some critical value, here assumed to be $\varepsilon_{SPLIT} = \varepsilon_{UTS}$, with the corresponding CTOD parameter, $CTOD_{UTS}$. Further deformation leads to necking in the ligaments between the splits, until initiation of crack extension occurs where the height, H, of the splits is included in the integrated expression for $CTOD_i$ as given in equation 4). Correspondingly, the splits are spread ahead of the main crack front where the extent of splitting is assumed to be governed by the contour representing the strain at the ultimate tensile strength ε_{UTS}, when assuming ε_{UTS} to be the critical strain at initiation of splitting and localization. At initiation of stable crack growth, the split advance may be characterized by a length, L_s, ahead of the blunt crack tip. The subsequent stable growth regime will then include propagation of the main crack front as well as propagation of the splits ahead of the advancing crack. Localization through necking of the ligament between splits thus takes place within the contour of the splits ahead of the moving crack where the failure strain is reached at the main crack tip.

Rearranging the expression for the integrated initiation toughness by keeping the two parts of equation 2) separated, equation 3) becomes:

$$CTOD_i = \varepsilon_{UTSP} \; H + 2 \int_0^{H/2} (\varepsilon_{fPS} - \varepsilon_{UTSP}) \frac{x^3}{(H/2)^3} \, dx \qquad 7)$$

$$CTOD_i = H\varepsilon_{UTSP} + \frac{H}{4} (\varepsilon_{fPS} - \varepsilon_{UTSP}) \qquad 8)$$

$$CTOD_i = CTOD_{UTS} + CTOD_{LOC} \qquad 9)$$

Thus the initiation toughness includes two main factors, the $CTOD_{UTS}$ decribing the uniform deformation until the ultimate tensile strain is reached, and the $CTOD_{LOC}$ that represents the strain localization during the necking mechanism of the ligament. When the crack is growing, the process zone moves along ahead of the tip and the $CTOD_{LOC}$ represents the strain localization in the neck at the sharp crack, while the splits open within a distance l_s ahead of the main crack. The latter is schematically shown in fig 8 and demonstrated for the NVA-grade in fig 9. The $CTOD_{LOC}$ during stable growth is not physically measureable, but is an integrated measure of the strain during necking in the plane normal to the macroscopic crack plane intersecting the crack plane at the tip of the growing crack. For a continuously growing crack, a steady state strain controlled condition may be reached, the $CTOD_{LOC}$ is constant when assuming a constant failure strain at the crack tip, and $CTOD_{LOC}$ may be associated with the frequently used parameter $CTOD_a$. However, when the growing crack is sharp, which may be typical for ductile stable crack extension, Lereim (2), F.M. Beremin (18), there may be doubts about the meaning of $CTOD_a$.

On the other hand if the displacement is measured at a distance l_s behind the advancing crack, this might be the proper representation of a parameter $CTOD_a$. Correspondingly, the crack tip opening angle may the be characterized by:

$$CTOA = \frac{CTOD_a}{l_s} \qquad 10)$$

When assuming $CTOD_a \equiv CTOD_{LOC}$, the present model supports the work by Wnuk (19) and E. Smith (4,5) that the final stretch in the process zone and the crack tip opening angle are equivalent parameters for the characterization of

stable crack growth.

Derivation of the $CTOD_{LOC}$ from equation 8) leads to the data given in table 6. and $CTOD_{LOC}$ or $CTOD_a$ is in the range (.35 - .50) x $CTOD_i$. Thus, the steady state $CTOD_a$-representation is considerably smaller than the corresponding initiation toughness which is in agreement with the results of Garwood (20) where his constant value $CTOD_a$ was found to be approx. (.3 - .4) x $CTOD_i$. Although there may be uncertainties about the actual location of the $CTOD_a$ measurements relative to the real microscopic sharp crack front, it indicted that the present model is highly realistic.

However further studies are required in order to ascertain whether the present model of crack growth is quantitatively as weel as physically correct.

TABLE 6 - Initiation tougness $CTOD_i$, vs $CTOD_{LOC}$ representing the strain localisation during necking.

Grade	Orientation	$CTOD_i$	$CTOD_{LOC}$	$\frac{CTOD_{LOC}}{CTOD_i}$
NVA	TL	.258 H	.098 H	.38
	LT	.295 H	.105 H	.36
NVD	TL	.34 H	.16 H	.47
	LT	.4 H	.2 H	.5
NVE 36	TL	.325 H	.145 H	.44
	LT	.308 H	.118 H	.38

CONCLUDING REMARKS

For the orientations studied of rolled structural steels where splitting occurs the following may be concluded:

- The initiation fracture toughness $CTOD_i$ may be characterized by a model including the fracture strain under plane strain deformation, the characteristic distance which is a function of orientation and spacing between weak bands in the microstructure, and the total strain history in the necked ligaments between the splits.

- The stable crack growth is related to the fracture strain under plane strain deformation, the localized straining during necking and the split length l_s ahead of the growing crack.

Acknowledgements

The present study is financed by support from Det norske Veritas and The Royal Norwegian Council for Scientific and Industrial Research (NTNF).

The author also wishes to thank Mr. S. Slatcher for useful discussions.

REFERENCES

(1) R.F. Smith and J.F. Knott, Paper 69, pp 65 - 75, Proceedings Conference on "Practical Application of Fracture Mechanics to Pressure Vessel Tenchnology", May 1971, Instistute of Mech. Engineers.

(2) J. Lereim and J.D. Embury, pp 33- 53, "What does the Charpy Test really tell us" ed. A.R. Rosenfield, 1978. Proceedings of a sumposium held at the annual meeting of AIME/ASM. Denver, Colarado, U.S.A., February 1978.

(3) R. Iricibar, A. LeRoy and J.D. Embury, Metal Science, Aug. - Sept. 1980, Vol. 14 Nos 8 & 9, pp 327 - 336.

(4) E. Smith Trans. ASME Vol 103, April 1981, pp 148 - 150.

(5) E. Smith Int. J. of Fracture 17 (1981) pp 443 - 448.

(6) Det norske Veritas, January 1980, Rules for Classification of Steel Ships, Materials and Welding, Rolled Steel, Steel Tubes and Steel Forgings

(7) Lloyd's Register of Shipping, 1978, Rules and Regulations for the Construction and Classification of Ships.

(8) American Bureau of Shipping, 1980, Rules for Building and Classing Steel Vessels, Part 43, Materials for Hulls.

(9) D.P. Clausing, Internal Journal of Fracture Mechanics, Vol. 6, No. 1, March 1970, pp 71 - 85.

(10) British Standards Institution, BS5762: 1979, Methods for Crack Opening Displacement (COD) Testing.

(11) J.N. Robinson, Internation Journal of Fracture 12 (1976), pp 723 - 739.

(12) B.A. Fields and K.J. Miller, Engng Fracture Mechanics, 1977, 9, 137.

(13) J. Lereim and J.D. Embury, Engng Fracture Mechanics 11 (1979) pp 161 - 164.

(14) S. Slatcher. PhD Thesis. Univerity of Cambridge. To be published.

(15) A.A. Willoughby, P.L. Pratt and T.J. Baker. ICF 5, Cannes, France March 1981, Proceedings "Advances in Fracture Research" Ed. D. Francois Pergamon Press, pp 179 - 186.

(16) J. Lereim and S. Saether. "Fracture Resistance of Three Ship Steels". Presented at the Conference "Advances in Physical Metallurgy and Applications of Steels", Liverpool. September 1981.

(17) J.F. Knott. Metal Science Aug. - Sep. 1980, pp 327 - 336.

(18) F.M. Beremin. Proceedings "Three Dimensional Constitutive Relations and Ductile Fracture, Dourdan, France, June 1980. Ed. S. Nemat Nasser, North Holland Publishing Company.

(19) M.P. Wnuk. Int. J. of Fracture Vol 15, 1979, pp 553 - 582.

(20) S.J. Garwood and C.E. Turner. Int. Journ. of fracture 14 (1978), R 195 - 198.

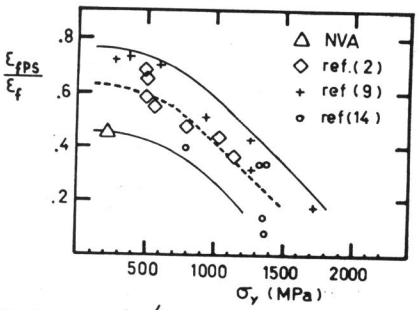

Fig. 1 Ratio of $\varepsilon_{fPS}/\varepsilon_f$ vs. yield strength

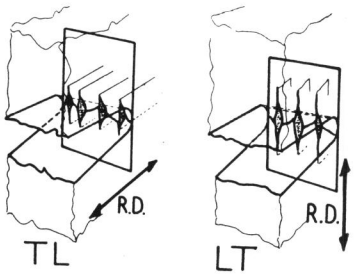

Fig. 2 Sketches of splitting or "tunnelling" occurring prior to initiation of stable crack growth at the tip of through thickness cracks.

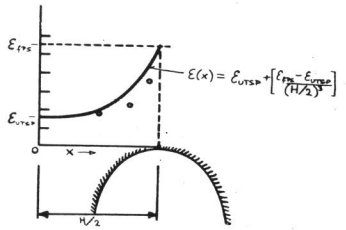

Fig. 3 Strain distribution to side of crack plane at initiation of stable growth where the split height H is assumed to represent a necked region in between bands of inclusions.

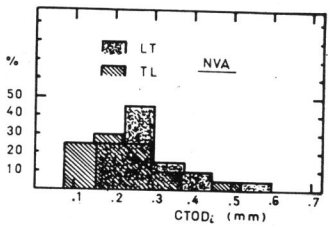

Fig. 4 Predicted variation of $CTOD_i$ according to variation in splitheight or corresponding ligament width for steel NVA.

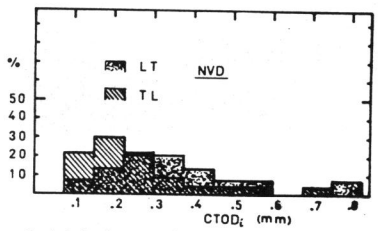

Fig. 5 Predicted variation of $CTOD_i$ according to variation in splitheight or corresponding ligament width for steel NVD.

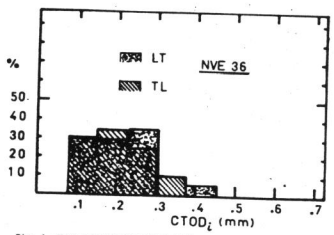

Fig. 6 $CTOD_i$-variation predicted from variation in splitheight or corresponding ligament width for steel NVE 36.

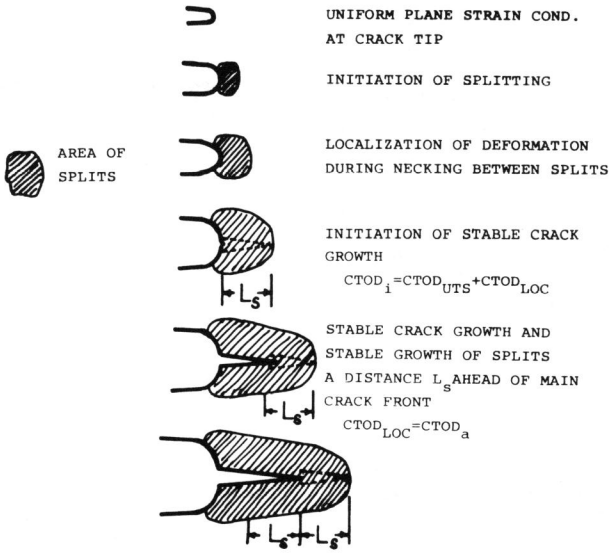

Fig. 7 Deformation history of a growing crack including splitting

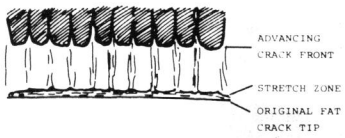

Fig. 8 Schematic illustration of a growing crack showing splitting a head of the main crack front in the crack plane

Fig. 9 Illustration of stable crack growth and corresponding splitting ahead of main crack front.Steel NVA.Micrograph in the crack plane.